Progress In Electromagnetics Research, Vol. 124, 301–314, 2012

DESIGN OF A TERAHERTZ POLARIZATION ROTATOR BASED ON A PERIODIC SEQUENCE OF CHIRAL-METAMATERIAL AND DIELECTRIC SLABS

C. Sabah* **and H. G. Roskos**

Johann Wolfgang Goethe-Universität, Physikalisches Institut, Max-von-Laue-Strasse 1, Frankfurt am Main D-60438, Germany

Abstract—The lack of wave-plates for the terahertz region opens the way for novel components/devices enabling polarization control at these frequencies. With the aid of chiral metamaterials — a new class of metamaterials — novel possibilities for the fabrication of multilayer structures for the realization of polarization rotators emerge. In this study, we present design and analysis of a polarization rotator for the terahertz frequency regime based on a multilayer structure consisting of an alternating sequence of chiral-metamaterial- and dielectric-plates. The combination of chiral constituents with dielectrics permits optimization of the spectral-filter and polarization-rotation features. We can generate either polarization-rotation combs or narrow rotation bands with very good and broad sideband suppression, of interest for example for data transmission or sensing purposes.

1. INTRODUCTION

Electromagnetic metamaterials (MTMs) are artificially structured composites that can be engineered to have desired electromagnetic properties, such as negative permittivity, negative permeability, artificial magnetism, negative refraction and/or negative reflection [1–3]. The materials are called single-negative metamaterials (SNG MTMs) if either the permittivity or the permeability is negative — but not both of them simultaneously — over a certain frequency band of interest. The term double-negative metamaterials (DNG MTMs) is used if both the permittivity and the permeability are simultaneously negative. Such DNG MTMs have been shown to significantly alter the properties of Bragg structures consisting of a sequence of DNG MTMs

Received 26 November 2011, Accepted 23 January 2012, Scheduled 27 January 2012

* Corresponding author: Cumali Sabah (Sabah@Physik.uni-frankfurt.de).

and conventional dielectric slabs [4–14], shifting the high-reflectance regions and providing broadened blocking bands, weaker incident-angle dependency, and vanishing secondary interference structures. If the dielectric and/or the DNG MTM layers are, in addition chiral, then the possibilities for design and performance variations of the configuration increase even further [15, 16]. The additional chirality parameter brings optical activity, circular dichroism, and polarization rotation to the system. Basically, chirality is defined as the geometric property of a structure of being non-superimposable onto its mirror image. When a MTM configuration is constructed from intrinsically chiral elements or contains properly structured artificial inclusions which introduce chirality, then it can be considered as a chiral MTM [1, 15–42]. Chiral MTMs are a new class of MTMs which offer negative refraction as well as cross-coupling between the electric and magnetic fields.

In this study, chiral multilayer structures formed by MTMs and dielectric slabs are investigated with the aim of designing a polarization rotator for the terahertz (THz) frequency regime. The incident THz wave is assumed to be a monochromatic wave with arbitrary polarization. The transfer matrix method is used in the analysis, the elements of the transfer matrix being expressed as a function of the angle of incidence, the structure parameters such as the thickness of each slab, and the frequency. Then, the power of the incident, reflected, and transmitted waves is determined and the power transmittance and reflectance specified for each structure. First, a conventional stratified Bragg structure will be considered as a reference. Then, the structure will be modified to form a combination of DNG MTM- and dielectric-layers to observe the effect of the DNG material on the reflection and transmission characteristics of the configuration. At last, chirality will be added to the configuration and the effect of the chirality be investigated. Note that equal optical thickness of each layer is considered in all our configurations. We find for this case that the thickness of the DNG layers drops out of the transmission function because of the boundary conditions for the transition between DNG MTMs and conventional dielectrics [13]. Consequently, the structure behaves as a classical Fabry-Perot resonator with highly reflecting surfaces. The results encourage the realization of polarization rotators which then could represent another prominent example for the use of MTMs in THz applications [38].

2. ELECTRODYNAMICS OF CHIRAL MEDIA

A chiral object is, by definition, a body that cannot be brought into congruence with its mirror image by translation and

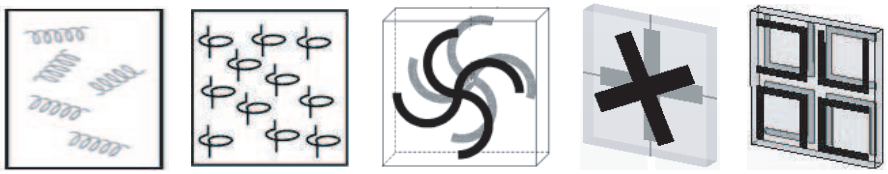

Figure 1. Examples of chiral structures. In analogy to the terminology in chemistry, one can call two chiral (mirror) compounds enantiomorphs, each of them being an enantiomer. Helicity (handedness) is one example of chirality. From left to right, chiral medium based on the random orientation of helical inclusions [17]; uniaxial chiral medium based on oriented wire helices [17]; enantiomeric helicoidal bilayered twisted rosettes [25, 27]; bilayered twisted cut-wire chiral MTM [30, 35, 41]; uniaxial chiral metamaterial constructed by double-layered four "U" split ring resonators [32, 42].

rotation [17, 18, 39]. Figure 1 shows some examples of chiral elements considered for use in MTMs.

A chiral medium provides a cross-coupling between the electric and magnetic fields. For a reciprocal and polarization-independent chiral medium, the constitutive relations can be written as follows:

$$\vec{D} = \varepsilon \cdot \vec{E} - i\kappa \cdot \vec{B} \tag{1a}$$

$$\vec{B} = \mu \cdot \vec{H} + i\kappa \cdot \vec{D} \tag{1b}$$

where ε is the permittivity, μ the permeability, and κ the chirality parameter. The latter is a complex quantity in which the real part determines the amount of cross-coupling (optical activity and polarization rotation) and the imaginary part determines the ellipticity (circular dichroism) [35]. The eigen-solutions of the electromagnetic waves in chiral media are the right-handed circularly polarized (RCP, $+$) wave and the left-handed circularly polarized (LCP, $-$) wave [20]. Their refractive indices are $n_{\pm} = n \pm \kappa$, respectively, with $n = \sqrt{\varepsilon \cdot \mu}$ [20, 35]. The indices for RCP and LCP waves hence differ by 2κ. If $|\kappa|$ is large, we have an alternative path to achieve a negative index [40]. In our case, $|\kappa|$, while being large enough for sufficient cross-coupling of the electric and magnetic fields, is generally small compared to $|n|$ and will not be used to achieve a sign change of the refractive index [20–22, 24, 26].

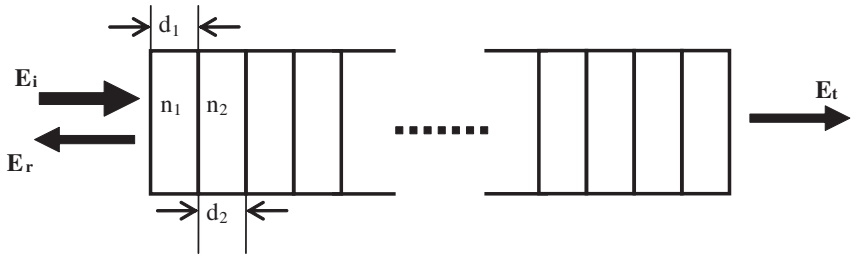

Figure 2. Schematic representation of the investigated stratified structure.

3. THEORETICAL ANALYSIS

In this section, the theoretical approach to investigate a planar multilayer structure (comprised of conventional dielectric, conventional chiral, DNG MTM, and chiral MTM layers with combinations thereof as specified later) to obtain high-reflection bands, high-transmission bands, and polarization rotation is presented. All computations are based on the theory of multilayer structures using the transfer matrix method [5–10]. For a generic multilayer structure (see Figure 2) embedded between two semi-infinite dielectric media, the transfer matrix formulation is given as:

$$\begin{bmatrix} E_{i\perp} \\ E_{r\perp} \\ E_{i//} \\ E_{r//} \end{bmatrix} = [U] \begin{bmatrix} E_{t\perp} \\ E_{t//} \end{bmatrix} = \begin{bmatrix} u_{11}\, u_{12} \\ u_{21}\, u_{22} \\ u_{31}\, u_{32} \\ u_{41}\, u_{42} \end{bmatrix} \begin{bmatrix} E_{t\perp} \\ E_{t//} \end{bmatrix} \tag{2}$$

where the subscripts // and $\perp$ refer to the parallel and perpendicular components of the electric field vector, respectively. Note that $[U] = [A][B_1][B_2][B_3] \ldots [B_m] \ldots [B_{N-1}][C]$. Here, the matrices $[B_m]$, $m = 1, 2, \ldots, N-1$, describe each of the layers, while $[A]$ and $[C]$ refer to the embedding dielectrics. $[A]$ and $[B_m]$ are square matrices of order 4, $[C]$ is a 4×2 matrix and $[U]$ correspondingly is also a 4×2 matrix. RCP and LCP waves are used as the eigen-functions and the surrounding medium is assumed to be air in the numerical calculations. Note that the conservation of the power is fulfilled in all computations.

4. NUMERICAL RESULTS

In this section, the numerical results for four different cases will be presented. All four investigated structures are composed of five

alternating layers constituting stacks of the form $XDXDX$. The second and fourth layers, denoted as D, are of the same dielectric material with the refractive index of 2.2 (representing zirconium oxide [43]) and remain unchanged. The other three layers, denoted as X are being varied. In the first case, X stands for a conventional dielectric, then we consider a conventional chiral dielectric, then a DNG MTM, and finally a chiral DNG MTM. It is assumed that the absolute value of the refractive index is 4.6 (representing tellurium [43]), and that the influence of the chirality parameter on the index is insignificant (see later). The optical thickness ($|n_m| \times d_m$) of all layers is arranged to be $\lambda_0/4$ where λ_0 is the free-space wavelength at the operation frequency (1.0 THz). All computations are performed for an incident electric field with p-polarization ($E_{i\perp} = 0$). Note that, in order to verify the computations, the conservation of power is tested and found to be satisfied for all examples. As a second test method, a transmission line equivalent is obtained for the structure given in Figure 2 which is then evaluated numerically following the procedure described in Refs. [5, 44]. Both methods give the same numerical values for all computations.

For the first structure, the all-dielectric one, the power reflection and transmission characteristics are expected to be those of a conventional interference filter This is confirmed by the spectral data shown in Figure 3. The reflection (transmission) becomes unity

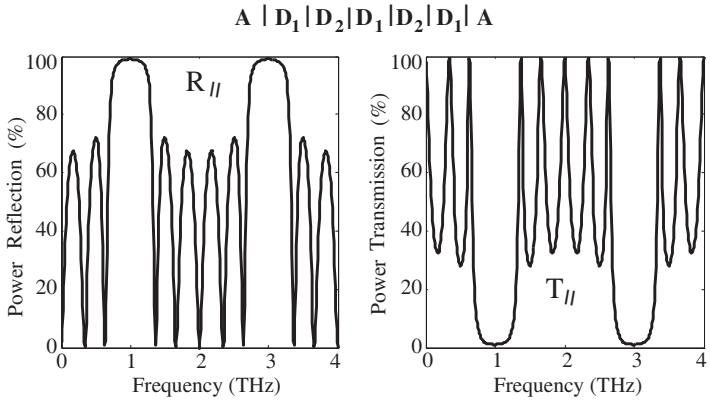

Figure 3. Frequency dependence of the power reflection (reflectance) and the power transmission (transmittance) of the five-layer all-dielectric structure. (The superscript schematically describes the layer sequence, with A: Air, D_1: first dielectric layer, and D_2: second dielectric layer).

(zero) at and around 1.0 THz and 3.0 THz with a bandwidth of these high-reflectance bands of 0.72 THz (bandwidth being defined as the frequency range of the amplitude wave above 70.7 % of the maximum points, 3 dB bandwidth). Multiple high-transmission lines surround the high-reflectance bands, the transmittance nearly reaching unity at 0, 0.34, 0.64, 1.36, 1.66, 2.0 THz and then again at 2.34, 2.64, 3.36, 3.66, 4.0 THz. The corresponding reflectance is very close to zero at these frequencies. Note that the perpendicular component of the power reflection and transmission is zero since the structure is excited by a p-polarized electric field. As a result, the structure behaves as a high-reflection band-pass filter or high-reflection coating at 1.0 and 3.0 THz, while it acts as narrow-band anti-reflection (full-transmission) filter at a multitude of other frequencies.

Coming to the second case, the five-layer structure now contains a double-positive chiral medium as the X material. It has the same refractive index of 4.6 as in the case considered before, but with the additional chirality parameter of -2×10^{-3}. Its value is so small that its influence on the refractive index is negligible. Note that the chirality parameter is carefully selected and its absolute value has to be lower than the upper bound resulting from maximum coupling and given by $|\kappa| \leq \sqrt{\varepsilon/\mu}$ where ε and μ are permittivity and permeability of the medium [17–20]. We chose the optimum value for our study to provide sufficient coupling between the electric and magnetic fields. Note those Refs. [17, 19] emphasize that even a small value of κ can have a pronounced effect on the transmitted wave through rotation of the polarization. Note again, for the selected optimum chirality value, there exists a perfect symmetry in the power reflection and transmission with respect to the operation frequency but the symmetry can be lost for different chirality values [20]. Figure 4 shows the power reflection and transmission as a function of frequency. For the reflection, identical results are obtained as in the previous case. The structure acts as a band-pass filter and a high-reflection coating for frequencies at and around 1.0 THz and 3.0 THz. However, the transmission behavior is drastically altered. The chirality now leads to a polarization-rotated transmitted wave (while this special structure does not support a polarization-rotated reflected wave). The p-polarized component of the transmission is now decreased (and is weak from 0.8 to 3.2 THz) in comparison with the previous case, and it reaches close to zero at 2.0 THz. At the same time, the perpendicularly polarized component of the transmitted wave has a high transittance over a large region between 1 and 3 THz, and it nearly reaches unity at 2.0 THz, although the incident electric field has no perpendicular component at all (optical activity and polarization

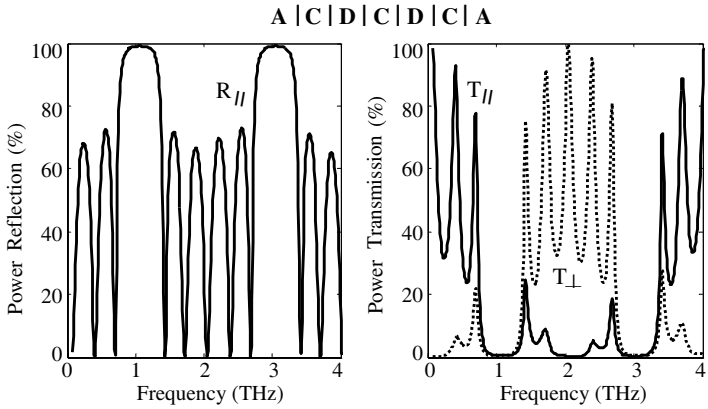

Figure 4. Power reflection and transmission as a function of frequency for five layers of chiral-dielectric structure (A: Air, C: Chiral (conventional or double-positive), and D: Dielectric).

rotation with 100% efficiency at 2.0 THz and multiples thereof). At this frequency a complete parallel-to-perpendicular polarization conversion occurs for the transmitted wave. Therefore, one can say that the second structure acts as a polarization-conversion transmission filter in some THz frequency band. Note that there are also pronounced frequency oscillations (ripples) in the reflection and transmission data as in the previous example.

As a third example, a five-layer structure is investigated as in the first two cases, but here the medium X is arranged to be a DNG-MTM with a refractive index of -4.6. The power reflection and transmission versus frequency are shown in Figure 5. In this case, the pass-bands are wider in comparison with the previous examples (broad high-reflection bands). The reflection and transmission spectra show only one high-transmission peak per high-reflection band, i.e., the spectra exhibit no ripples as in the previous two cases. The present structure can be described as a narrow-band transmission filter with excellent rejection outside the pass-bands.

The disappearance of the ripples is entirely a consequence of the boundary conditions, as is explained in Secetion 3 of Ref. [13]. While the continuity of the electric and magnetic fields at the boundaries of layers leaves the interface reflection and transmission coefficients unchanged if a dielectric medium is replaced by a DNG material with the same value on $|n_i|$, it demands a sign change of the phase term because the wave propagates in the opposite direction. This leads to cancellation of fast-oscillating terms.

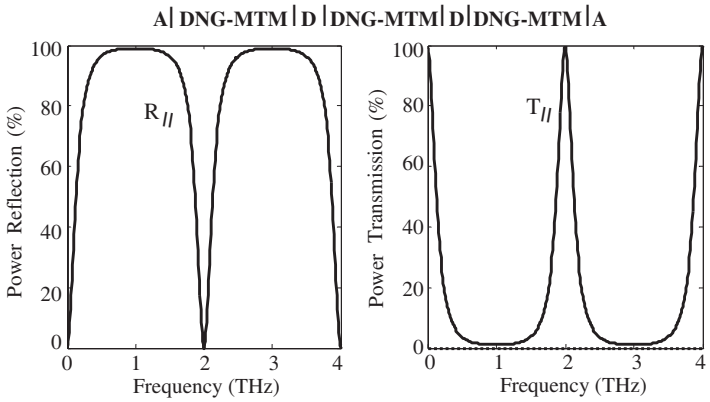

Figure 5. Power reflection and transmission versus frequency for five-layer (DNG MTMs and dielectrics) structure (A: Air, DNG-MTM: Double-Negative Metamaterial, and D: Dielectric).

If we consider, for simplicity, a symmetric three-layer structure XDX embedded in air, then the ratio of the total field reflection coefficient (r) to the transmission coefficient (t) of the structure can be derived in a similar way as in Refs. [13, 43]. One obtains:

$$\frac{r}{t} \cong \frac{r_{ax}+r_{xa}\exp[\pm 2j\varphi_x]+r_{dx}\exp[2j(\pm\varphi_x\pm\varphi_d)]+r_{xd}\exp[2j(\pm\varphi_x\pm\varphi_d\pm\varphi_x)]}{t_{ax}t_{xd}t_{dx}t_{xa}\exp[j(\pm\varphi_x\pm\varphi_d\pm\varphi_x)]}. \quad (3)$$

Here, multiple reflections in the numerator have been neglected because of their small contribution [13, 43, 45]. The parameters r_{ij} and t_{ij} ($i = a,\ x,\ d$ and $j = a,\ x,\ d$) are the interface reflection and transmission coefficients; a, x, and d stand for air, medium X, and dielectric, correspondingly. Be reminded, that the interface reflection and transmission coefficients involve only the values of the refractive indices, but not the thicknesses of the layers. The phase terms are $\pm\varphi_{x,\,d} = \pm k_{x,\,d}d_{x,\,d}$, they contain the frequency and thickness dependence. The plus-signs refer to DNG MTMs, and the minus-signs to dielectrics.

Only for sequences of DNG MTMs and dielectrics, but not for all-dielectric layers, Eq. (3) simplifies to:

$$\frac{r}{t} \cong \frac{r_{ax} + r_{xa}\exp(+j2\varphi_x) + r_{dx} + r_{xd}\exp(+j2\varphi_x)}{t_{ax}t_{xd}t_{dx}t_{xa}\exp(+j\varphi_x)}. \quad (4)$$

Here, we have used the relations $r_{xa} = -r_{ax}$, $r_{xd} = -r_{dx}$, $t_{xa} = t_{ax}$, and $t_{xd} = t_{dx}$. We can now follow the argumentation of Ref. [13] and compare the frequency behavior of a pure stack of dielectrics with our sequence of DNG MTM and conventional dielectric media. In

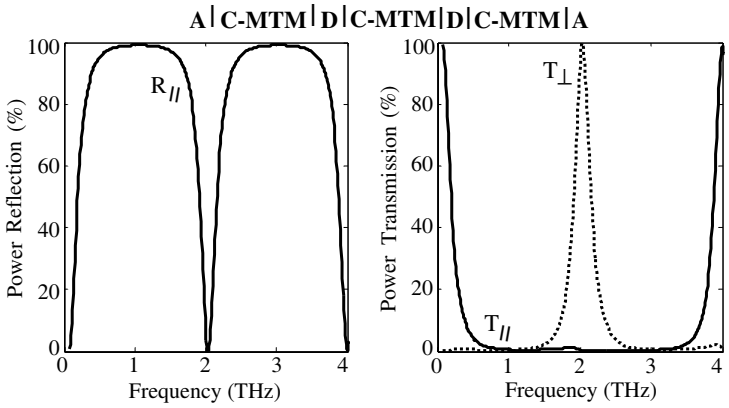

Figure 6. Power reflection and transmission against the frequency for five-layer (chiral MTMs-dielectrics) structure (A: Air, C-MTM: Chiral Metamaterial, and D: Dielectric).

the case of all-dielectric stacks, Eq. (3) will result in a fast-oscillating frequency dependence (cf. ripples in Figure 3). The expression of Eq. (4), in contrast, is simpler, with the phase terms, which contain several summands and are responsible for the fast oscillations, gone. Interestingly, each of the remaining phase terms contains only the thickness of medium X. Remarkably, Eq. (4) has the structure of the corresponding expression of a Fabry-Perot filter. The DNG MTM takes on the role of the dielectric of the Fabry-Perot filter, while the dielectric of our structure plays the role of the reflective coating of the Fabry-Perot. Only the refractive index of this "dielectric-layer coating" is of significance for the Fabry-Perot's electromagnetic response, not its thickness.

At last, the five-layer structure composed of dielectric and chiral MTM (X medium) is analyzed. In this case, the chiral MTM has a refractive index of -4.6 and a chirality parameter of -2×10^{-3}. Figure 6 presents the reflection and transmission data. The reflection (with broad high-reflection bands) and transmission have the same ripple-free features as in the previous example. The parallel component of the transmission is minimized at around 2.0 THz and the perpendicular component has a high peak at this frequency. Complete polarization conversion occurs at 2.0 THz. This means that broad spacing of transmission maxima retained, but only every second maximum transmits at incoming polarization. For other transmission maxima, polarization rotation arises.

5. DISCUSSION

One important issue to be discussed with a view towards the practical realization of a polarization rotator is the dispersion character of both the refractive index and the chirality of the chiral MTM. In general, they possess a frequency-dependent nature in such structures. However, it is found that they exhibit a flat behavior in certain frequency regions [26–42] which makes our proposal feasible. Another important issue is the effect of losses of the chiral MTM structures. The loss arising in these kinds of structures usually comes from the metallic inclusions and the dielectric substrate used. Nevertheless, one can minimize the effect of loss by proper selection of the metal and substrate [27–42]. For example, quartz glass can be chosen as a substrate for its moderately low loss and transparency properties in the THz range. In addition, silver can be used for congruent metallization in the same frequency region. The number of examples can be increased.

6. CONCLUSION

The frequency response of periodic multilayer structures composed of four different combinations of materials, dielectric, chiral, DNG-MTM, and chiral MTM, is presented. The optical activity, interference filtering, high-reflection coating, polarization rotation features of structures with optimized parameters (notably the chirality parameter) for the THz region are presented via numerical results. DNG MTM slabs increase the high-reflection regions and decrease or let vanish the multitude of transmission maxima such that only one transmission maximum survives per reflection maximum. The structure with chiral MTM slabs has the same features with additional polarization rotation for every second transmission maximum. Consequently, the proposed structure can be utilized for filtering, coating, and especially polarization conversion devices in the THz regime. As a result, this study — as a conceptual work — paves the way towards the realization of a THz polarization rotator by designing a chiral MTM with the desired parameters which is feasible using the current technology with the sophisticated fabrication processes [27–42].

REFERENCES

1. Sihvola, A., "Electromagnetic emergence in metamaterials," *Advances in Electromagnetics of Complex Media and Metamaterials*, S. Zouhdi, A. Sihvola, and M. Arsalane (eds.), Vol. 89, *NATO*

Science Series II: Mathematics, Physics, and Chemistry, Kluwer Academic, 2003.

2. Engheta, N. and R. W. Ziolkowski, *Metamaterials: Physics and Engineering Explorations*, Wiley-IEEE Press, Piscataway, NJ, 2006.
3. Solymar, L. and E. Shamonina, *Waves in Metamaterials*, Oxford University Press, New York, 2009.
4. Zhou, L., W. Wen, C. T. Chan, and P. Sheng, "Electromagnetic wave tunneling through negative-permittivity media with high magnetic fields," *Phys. Rev. Lett.*, Vol. 94, 243905, 2005.
5. Sabah, C., *Analysis, Applications, and a Novel Design of Double Negative Metamaterials*, Ph.D. Thesis, Gaziantep, Turkey, 2008.
6. Sabah, C. and S. Uckun, "Physical features of left-handed mirrors in millimeter wave band," *J. Optoelectron. Adv. Mater.*, Vol. 9, 2480–2484, 2007.
7. Sabah, C. and S. Uckun, "Scattering characteristics of the stratified double-negative stacks using the frequency dispersive cold plasma medium," *Zeitschrift für Naturforschung A*, Vol. 62a, 247–253, 2007.
8. Sabah, C. and S. Uckun, "Frequency response of multilayer media comprised of double-negative and double-positive slabs," *Chinese Phys. Lett.*, Vol. 24, 1242–1244, 2007.
9. Sabah, C. and S. Uckun, "Multilayer system of lorentz/drude type metamaterials with dielectric slabs and its application to electromagnetic filters," *Progress In Electromagnetics Research*, Vol. 91, 349–364, 2009.
10. Sabah, C., "Numerical study of high reflection coatings with negative and positive refractive indexes," *Optoelectron. Adv. Mater.-R.C.*, Vol. 3, 860–864, 2009.
11. Gerardin, J. and A. Lakhtakia, "Negative index of refraction and distributed Bragg reflectors," *Microw. Opt. Tech. Lett.*, Vol. 34, 409–411, 2002.
12. Wu, L., S. He, and L. Chen, "On unusual narrow transmission bands for a multilayered periodic structure containing left-handed materials," *Opt. Express*, Vol. 11, 1283–1290, 2003.
13. Cory, H. and C. Zach, "Wave propagation in metamaterial multilayered structures," *Microw. Opt. Tech. Lett.*, Vol. 40, 460–465, 2004.
14. Engheta, N. and R. W. Ziolkowski, "A positive future for double-negative metamaterials," *IEEE Trans. Microw. Theory Tech.*, Vol. 4, 1535–1556, 2005.

15. Sabah, C. and H. G. Roskos, "Periodic array of chiral metamaterial-dielectric slabs for the application as terahertz polarization rotator," *XXXth URSI General Assembly and Scientific Symposium*, Istanbul, Turkey, 2011.
16. Sabah, C. and H. G. Roskos, "Terahertz polarization rotator consists of chiral metamaterial and dielectric slabs," *IRMMW-THz*, Houston, TX, USA, 2011.
17. Jaggard, D. L., A. R. Mickelson, and C. H. Papas, "On electromagnetic waves in chiral media," *Appl. Physics*, Vol. 18, 211–216, 1979.
18. Engheta, N. and D. L. Jaggard, "Electromagnetic chirality and its applications," *IEEE AP-S Newsletter*, Vol. 30, 6–12, 1988.
19. Jaggard, D. L., N. Engheta, M. W. Kowarz, P. Pelet, J. C. Liu, and Y. Kim, "Periodic chiral structures," *IEEE Trans. Antennas Propag.*, Vol. 37, 1447–1452, 1989.
20. Sabah, C. and S. Uckun, "Reflection and transmission coefficients of multiple chiral layers," *Sci. China Ser. E: Tech. Sci.*, Vol. 49, 457–467, 2006.
21. Jin, Y. and S. He, "Focusing by a slab of chiral medium," *Opt. Express*, Vol. 13, 4974–4979, 2005.
22. Agranovich, V. M., Y. N. Gartstein, and A. A. Zakhidov, "Negative refraction in gyrotropic media," *Phys. Rev. B*, Vol. 73, 045114, 2006.
23. Rogacheva, A. V., V. A. Fedotov, A. S. Schwanecke, and N. I. Zheludev, "Giant gyrotropy due to electromagnetic-field coupling in a bilayered chiral structure," *Phys. Rev. Lett.*, Vol. 97, 177401, 2006.
24. Mackay, T. G. and A. Lakhtakia, "Simultaneous negative- and positive-phase-velocity propagation in an isotropic chiral medium," *Microw. Opt. Tech. Lett.*, Vol. 49, 1245–1246, 2007.
25. Plum, E., V. A. Fedotov, A. S. Schwanecke, N. I. Zheludev, and Y. Chen, "Giant optical gyrotropy due to electromagnetic coupling," *Appl. Phys. Lett.*, Vol. 90, 2231131, 2007.
26. Sabah, C., "Left-handed chiral metamaterials," *Cent. Eur. J. Phys.*, Vol. 6, 872–878, 2008.
27. Plum, E., V. A. Fedotov, and N. I. Zheludev, "Optical activity in extrinsically chiral metamaterial," *Appl. Phys. Lett.*, Vol. 93, 191911, 2008.
28. Kwon, D.-H., P. L. Werner, and D. H. Werner, "Optical planar chiral metamaterial designs for strong circular dichroism and polarization rotation," *Opt. Express*, Vol. 16, 11802–11807, 2008.

29. Kwon, D. H., D. H. Werner, A. V. Kildishev, and V. M. Shalaev, "Material parameter retrieval procedure for general bi-isotropic metamaterials and its application to optical chiral negative-index metamaterial design," *Opt. Express*, Vol. 16, 11822–11829, 2008.
30. Wang, B., J. Zhou, T. Koschny, M. Kafesaki, and C. M. Soukoulis, "Chiral metamaterials: Simulations and experiments," *J. Opt. A: Pure Appl. Opt.*, Vol. 11, 114003, 2009.
31. Zhang, S., Y. S. Park, J. Li, X. Lu, W. Zhang, and X. Zhang, "Negative refractive index in chiral metamaterials," *Phys. Rev. Lett.*, Vol. 102, 023901, 2009.
32. Xiong, X., W. H. Sun, Y. J. Bao, M. Wang, R. W. Peng, C. Sun, X. Lu, J. Shao, Z. F. Li, and N. B. Ming, "Construction of a chiral metamaterial with a U-shaped resonator assembly," *Phys. Rev. B*, Vol. 81, 075119, 2010.
33. Ye, Y. and S. He, "90° polarization rotator using a bilayered chiral metamaterial with giant optical activity," *Appl. Phys. Lett.*, Vol. 96, 203501, 2010.
34. Wu, Z., B. Q. Zeng, and S. Zhong, "A double-layer chiral metamaterial with negative index," *Journal of Electromagnetic Waves and Applications*, Vol. 24, No. 7, 983–992, 2010.
35. Zhao, R., T. Koschny, and C. M. Soukoulis, "Chiral metamaterials: Retrieval of the effective parameters with and without substrate," *Opt. Express*, Vol. 18, 14553–14567, 2010.
36. Li, J., F.-Q. Yang, and J. Dong, "Design and simulation of L-shaped chiral negative refractive index structure," *Progress In Electromagnetics Research*, Vol. 116, 395-408, 2011.
37. Canto, J. R., C. R. Paiva, and A. M. Barbosa, "Dispersion and losses in surface waveguides containing double negative or chiral metamaterials," *Progress In Electromagnetics Research*, Vol. 116, 409–423, 2011.
38. Withayachumnankul, W. and D. Abbott, "Metamaterials in the terahertz regime," *IEEE Phot. Journal*, Vol. 1, 99–118, 2009.
39. Decker, M., M. W. Klein, M. Wegener, and S. Linden, "Circular dichroism of planar chiral magnetic metamaterials," *Opt. Letters*, Vol. 32, 856–858, 2007.
40. Pendry, J. B., "A chiral route to negative refraction," *Science*, Vol. 306, 1353–1355, 2004.
41. Zhou, J., J. Dong, B. Wang, T. Koschny, M. Kafesaki, and C. M. Soukoulis, "Negative refractive index due to chirality," *Phys. Rev. B*, Vol. 79, 121104, 2009.

42. Li, Z., R. Zhao, T. Koschny, M. Kafesaki, K. B. Alici, E. Colak, H. Caglayan, E. Ozbay, and C. M. Soukoulis, "Chiral metamaterials with negative refractive index based on four "U" split ring resonators," *Appl. Phys. Lett.*, Vol. 97, 081901.1–081901.3, 2010.
43. Orfanidis, S. J., *Electromagnetic Waves and Antennas*, ece.rutgers.edu/∼orfanidi/ewa/.
44. Sabah, C., "Transmission line modeling method for planar boundaries containing positive and negative index media," *IEEE MMET'08 Conference Proceedings*, Odessa, Ukraine, 2008.
45. Kong, J. A., "Electromagnetic wave interaction with stratified negative isotropic media," *Progress In Electromagnetics Research*, Vol. 35, 1–52, 2002.